

# A simultaneous small- and wide-angle X-ray scattering study of the early stages of melt crystallization in polyethylene

Z.-G. Wang<sup>a</sup>, B.S. Hsiao<sup>a,\*</sup>, E.B. Sirota<sup>b</sup>, S. Srinivas<sup>c</sup>

<sup>a</sup>Department of Chemistry, State University of New York at Stony Brook, Stony Brook, NY 11794-3400, USA

<sup>b</sup>ExxonMobil Research and Engineering Company, Corporate Strategic Research, Annandale, NJ 08801, USA

<sup>c</sup>ExxonMobil Chemical Company, Baytown Polymers Center, Baytown, TX 77522-5200, USA

Received 4 October 1999; received in revised form 8 February 2000; accepted 14 February 2000

---

## Abstract

The early stages of isothermal melt crystallization in linear polyethylene (PE) were investigated via simultaneous synchrotron small-angle X-ray scattering (SAXS) and wide-angle X-ray diffraction (WAXD) techniques. During these stages, noticeable short-range density fluctuations with periodic spacing from 40 to 80 nm were detected (by SAXS) before the identification of three-dimensional crystal ordering (by WAXD). These results are consistent with the recent findings in several other polymers (polypropylene, poly(aryletherketone), poly(ethylene terephthalate) and poly(butylene terephthalate) by our and other laboratories. Some groups have proposed that the spinodal decomposition due to chain conformation in the molten state may act as a precursor to crystallization based on these findings. Detailed examination of the SAXS and WAXD data, however, indicated that the early stages of crystallization also follow the classical nucleation and growth behavior with a simple Avrami expression. The earlier detection of density fluctuations can be attributed to the lower detection limit of crystallinity in SAXS (0.1%) than in WAXD (1%). In addition, we found that the long spacing associated with the SAXS peak decreased slightly with time, which opposed the behavior of the spinodal decomposition. © 2000 Elsevier Science Ltd. All rights reserved.

**Keywords:** Melt crystallization; Polyethylene; Synchrotron

---

## 1. Introduction

Recently, several new findings using small-angle X-ray scattering (SAXS) and wide-angle X-ray diffraction (WAXD) to examine the early stages of crystallization in the quiescent state have provoked viewpoints that challenge the conventional belief of polymer crystallization through nucleation and growth processes. For example, during cold crystallization of quenched amorphous poly(ethylene terephthalate) (PET) and poly(aryletherketoneketone) (PEKK) samples, it was found that the SAXS peak appeared before WAXD crystalline reflections [1–6]. As the SAXS peak can be attributed to some form of density fluctuations (5–40 nm) and WAXD crystalline peaks are due to three-dimensional (3D) crystal ordering (0.2–1 nm), the occurrence of SAXS prior to WAXD suggests that density fluctuations take place before crystallization. Furthermore, the initial behavior of the SAXS data appears to be consistent with the Cahn–Hilliard theory for the spinodal

decomposition [7,8] (the peak position remains constant whereas the intensity grows exponentially with time). The recent studies of isotactic polypropylene (*i*PP) [9–11], and poly(butylene terephthalate) (PBT) [12] indicated that this behavior also held true for polymer crystallization in the molten state. It appeared that these density fluctuations, consistent with the spinodal decomposition behavior, might act as a precursor to crystallization in both solid and molten states. The spinodal decomposition behavior has been explained recently by Olmsted et al. as due to the coupling of density and chain conformation in the supercooled melt [13]. In our opinion, the hypothesis of the spinodal decomposition in the quenched glass may be rationalized in that the solid can retain a large degree of non-equilibrium structures and slow relaxation times. But the suggestion of the spinodal decomposition in the pre-crystallizing melt highly due to the aggregation of chain conformation is contested as the chain relaxation times can be very fast in the molten state ( $\ll 1$  s).

We realize that before we ponder the hypothesis of the spinodal decomposition as a precursor to crystallization, we must first evaluate if the same data deviate from the conventional nucleation and growth process. Recently, we have

---

\* Corresponding author. Tel.: +1-516-632-7793; fax: +1-516-632-6518.

E-mail address: bhsiao@notes.cc.sunysb.edu (B.S. Hsiao).

carried out such a study on *i*PP and concluded that the crystallinity development in the early stages of crystallization can be described also by a simple Avrami expression [11], which means that the initial structural development during crystallization is also consistent with the nucleation and growth behavior. In this study, we intend to further investigate if this is the case in polyethylene (PE). We have chosen two linear PE samples with different molecular weights and a narrow molecular weight distribution for this purpose.

We realize that the difficulties in probing the early stages of crystallization are the weak signals from the small volume fraction involved, combined with the detection limits (minimum detectable crystallinity) of the SAXS and WAXD techniques. In the previous study, we reported that the detection limits between SAXS and WAXD were quite different [11]. Using solutions of *n*-paraffin ( $C_{33}H_{68}$ ) in dodecane ( $C_{12}H_{26}$ ) at different concentrations as a model, the detection limit of WAXD was determined to be about 1%. In these solutions, the precipitated fraction simulated the degree of crystallinity in PE since the *n*-paraffin formed complete crystals and dodecane remained liquid at the measurement temperature. This method, however, could not resolve the detection limit of SAXS as the size of the crystal (in microns) was beyond the spatial resolution of the SAXS technique and very different from the PE lamellar thickness. We also showed that by using the time-resolved data itself (*i*PP), we could estimate the detection limits of the different techniques (SAXS, WAXD and light scattering) [11]. The detection limit of the WAXD technique determined by this method appeared to be the same as the model solution study.

Because the detection limits of SAXS and WAXD are different, merely comparing the first appearance of SAXS and WAXD intensities may not provide meaningful information. To illustrate the effects of signal-to-noise ratio and the detection limit on the detection of the crystallinity, we have modeled the induction period using a simple Avrami model [14] (with  $t = 0$ , i.e. without any induction time) to represent the nucleation and growth process [11]. We found that the apparent induction times can be manifested by the experimental artifacts such as sensitivity and detection limitations due to statistics and noise. This is because, an experimentally determined induction time is not the time when crystallinity exceeds zero, but rather when it exceeds some finite fraction, which will be set by the specific measurement. For example, using an Avrami exponent of 2.5, a time constant ( $\tau$ ) of 16,000 s, no induction time (with  $t = 0$ ), and three varying degrees of noise: 1, 0.1, and 0.01%, we have yielded three different values of apparent 'onset times' using the interception method from the linear plot of crystallinity and time [11].

The objective of this study is to evaluate if the initial development of the crystallinity, as measured by WAXD as well as SAXS, has deviated from the classic theory of nucleation and growth, such as some simple form of the

Avrami equation. The detection limits of SAXS and WAXD estimated in this study will be compared to the earlier model study [11].

## 2. Experimental

### 2.1. PE samples and preparation

The fractionated linear PE samples (SRM 1483 and 1484) were supplied by the National Institute of Standards and Technology (NIST). The SRM 1483 and 1484 samples were prepared at the NIST by a large-scale gel permeation chromatography from a linear whole PE (SRM 1475) with a broad molecular weight distribution. SRM 1483 had number- and weight-average molecular weights,  $M_n$  and  $M_w$ , of 28,900 and 32,100, respectively, and a polydispersity ( $M_w/M_n$ ) of 1.1 (designated as 32 K PE in this paper). SRM 1484 had number- and weight-average molecular weights,  $M_n$  and  $M_w$ , of 100,500 and 119,600, respectively, and a polydispersity ( $M_w/M_n$ ) of 1.2 (designated as 120 K PE in this paper). The theoretical equilibrium melting temperature ( $T_m^0$ ) for the 32 K PE is 143.65°C, and for the 120 K PE is 144.95°C. The samples were molded into void-free disks (7 mm in diameter) with thickness of 1.5 mm for X-ray measurements.

### 2.2. X-ray characterization techniques

Simultaneous SAXS and WAXD measurements were carried out at the Advanced Polymers Beamline (X27C,  $\lambda = 1.307 \text{ \AA}$ ) in the National Synchrotron Light Source (NSLS), Brookhaven National Laboratory (BNL). The details of the experimental setup at the X27C beamline have been reported elsewhere [15]. Two linear position sensitive detectors (made by the European Molecular Biological Laboratory, EMBL) were used to detect the simultaneous SAXS and WAXD signals. The sample to detector distance for the SAXS detection was 1950 mm, and for the WAXD detection was 110 mm. The SAXS profile was calibrated with silver behenate and duck tendon; the WAXD profile was calibrated with a silicon standard.

Isothermal melt crystallization was performed using a dual-chamber temperature jump apparatus, which has been described previously [16]. The sample was equilibrated first at 155°C for 5 min, then pneumatically 'jumped' to the lower temperature chamber for time-resolved simultaneous SAXS and WAXD measurements. In this study, four isothermal crystallization temperatures,  $T_{cs}$ , were chosen: 126.0, 128.6, 129.0°C, and 129.8°C. Note that the crystallization temperatures used are relatively high, which resulted in a long 'induction time' during the measurement. For example, 32 K PE has an induction time about 1200 s at 129.0°C. The time to reach the equilibrium measurement temperature after the temperature jump was less than 100 s. The initial 90% of the temperature change occurred at a rate of about 300°C/min. At the thermal

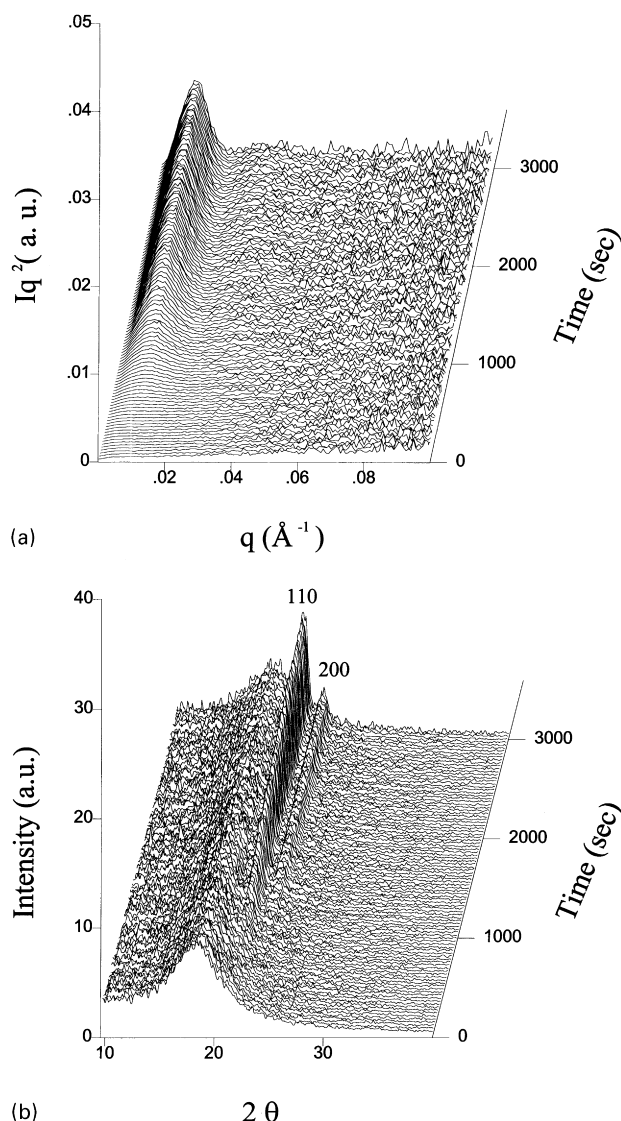


Fig. 1. Simultaneous (a) SAXS; (b) WAXD profiles collected during isothermal crystallization of 32 K PE at 128.6°C.

equilibrium, temperature fluctuations were less than  $\pm 0.3^\circ\text{C}$ . The data acquisition time for the X-ray measurement was 30 s/scan.

### 2.3. Data analysis

Proper analysis of the SAXS data depends upon the state of the material. Since we know little about the early stages of crystallization, the scattering data collected at the early stages of crystallization have been considered by several methods. All the SAXS data are corrected first by the Lorentz factor ( $I(q)q^2$ ,  $q = (4\pi/\lambda) \sin \theta$  with  $2\theta$  being the scattering angle) since the scattering system is isotropic [17]. As we find that the scattering profile exhibits a discrete peak, the data can be considered by the analyses of (1) the Cahn–Hilliard theory [7,8] assuming that the scattering maximum possesses the characteristics of the spinodal

decomposition, i.e. the peak intensity increases exponentially with time and the peak position remains constant; and (2) the correlation function analysis assuming that the peak arises from finite lamellar stacks [18,19].

From the WAXD profile, the peak position, peak height, peak width, and integrated intensity, for each crystal reflection and amorphous background can be extracted using a custom code capable of dealing with time resolved spectra. A Gaussian peak riding on a polynomial is used to fit the amorphous background; all other reflection peaks are fitted also with Gaussian functions. By dividing the total intensities of the crystalline reflections  $I_c$  to the overall intensity  $I_{\text{total}}$ , a measure of the mass fraction of the crystalline phase ( $\phi_{\text{mc}}$ ) in the sample can be obtained. Because of the possible defects in the crystal lattice and thermal disorder, the measured value of  $I_c$  must be lower than the true value. We note that by using this deconvolution method, the sample is assumed to possess two ideal phases (crystalline and amorphous), which is the criterion to define the term ‘crystallinity’ [19]. Since the crystal reflection signals are extremely weak in the early stages of crystallization, the determination of the crystallinity is stopped when the crystal reflection (110) cannot be isolated. Furthermore, as the ratio between the diffraction intensities of (110) and (200) is almost constant, we can assume that (200) also contributes to the crystallinity based on this ratio when only the (110) reflection is detected.

### 3. Results and discussion

Typical time-resolved SAXS and WAXD profiles obtained simultaneously during isothermal crystallization of 32 K PE at 128.6°C are shown in Fig. 1a and b, respectively. The low degree of supercooling ( $T_c = 128.6^\circ\text{C}$ ,  $\Delta T = 15.1^\circ\text{C}$ ) results in a slow crystallization rate, allowing the detailed examination of simultaneously collected SAXS and WAXD profiles. Simultaneous SAXS and WAXD profiles of 120 K PE collected at the same crystallization temperature ( $\Delta T = 16.4^\circ\text{C}$ ) are shown in Fig. 2a and b, respectively. The Lorentz corrected intensities are used in these SAXS profiles because the scattering system was measured by a linear detector [19]. Both SAXS profiles show the development of a discrete scattering maximum with time. The corresponding WAXD profiles show the evolution of two crystal reflections (110) and (200) with time.

Selected time-resolved SAXS and WAXD profiles of 32 K PE at 128.6°C are shown in Fig. 3a and b, respectively, to compare the kinetics of SAXS and WAXD developments. It is seen that a discrete SAXS peak first appears (marked by a bold line) at 480 s, and the crystalline reflections first become identifiable at about 660 s (also marked by a bold line). The determination of the initial SAXS peak here was based on the comparison of scattered intensity between the initial profile ( $t = 0$ ) and the profiles of different times at the

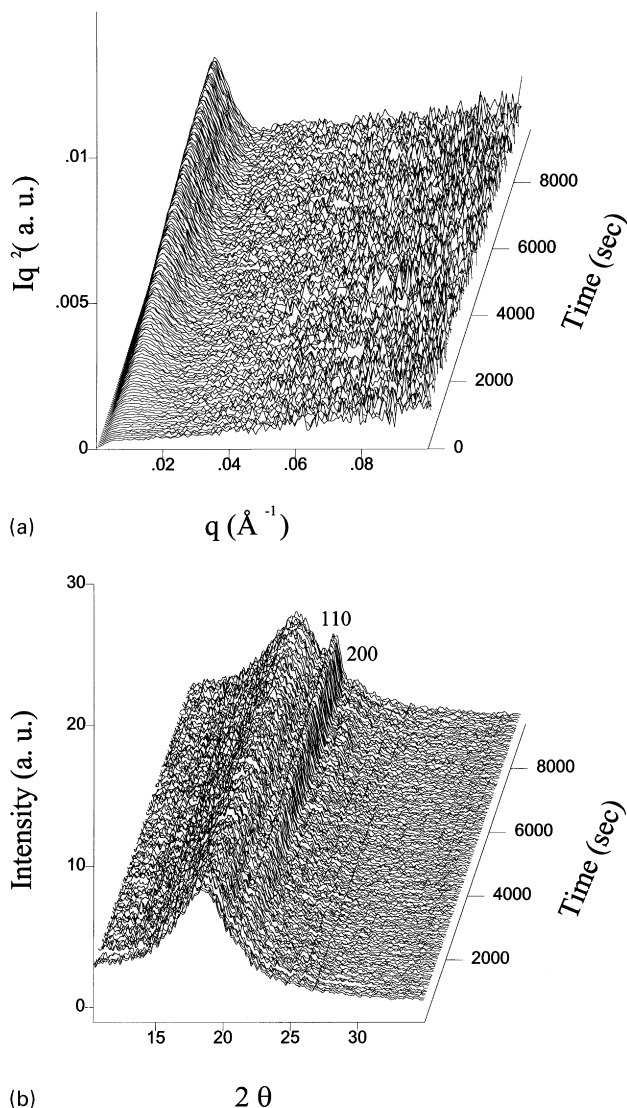
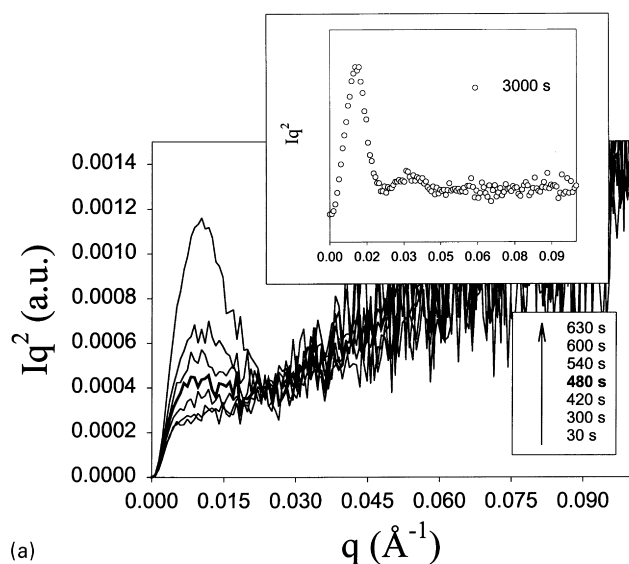


Fig. 2. Simultaneous (a) SAXS; (b) WAXD profiles collected during isothermal crystallization of 120 K PE at 128.6°C.

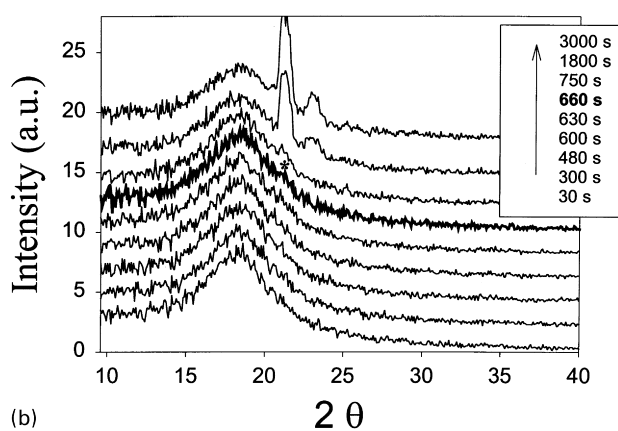
scattering maximum ( $q = 0.011 \text{ \AA}^{-1}$ ). The determination of the WAXD profile was based on the positive identification (signal-to-noise ratio  $S/N \geq 2$ ) of the strongest reflection (110) using the fitting routine. The time difference between the observation of the first SAXS peak (480 s) and the first WAXD crystal peak (660 s) is quite significant (180 s). This behavior is seen also in the higher molecular weight sample (120 K PE). Selected time-resolved SAXS and WAXD profiles of 120 K PE at 128.6°C are shown in Fig. 4a and b, respectively. It is seen that the time difference between the observation of the first SAXS peak (720 s) and the first WAXD crystal peaks (1380 s) is larger (660 s) than that of 32 K PE, even though a slightly greater degree of supercooling is encountered (by about 1°C). The slower crystallization kinetics in the higher molecular weight polymers have been documented broadly, which can be attributed to the lower chain mobility due to a greater degree of chain entanglements [20].

Ryan et al. [9,10] have used the interception method to determine the onset time for the initial peak appearance. We have compared the above method with the interception method. The time evolution profiles of both the invariant  $Q (= \int_0^\infty I(q)q^2 dq)$  [17,19] and the integrated intensity  $I_{\text{int}} (= \int_{q_1}^{q_2} I(q) dq)$  within the experimental  $q$  range ( $q_1 = 0.0035$  and  $q_2 = 0.25 \text{ \AA}^{-1}$ ) from 120 K PE at 128.6°C are shown in Fig. 5 (in linear scales). It is found that the onset time (determined by the slope change from the baseline) for both  $Q$  and  $I_{\text{int}}$  is about the same, which is similar also to the time determined from the method mentioned above at  $q = 0.011 \text{ \AA}^{-1}$  (Fig. 4). As discussed earlier, such onset times determined (termed apparent onset times) are not fundamental, a point on which we will elaborate later. The comparisons of the crystallinity  $\phi_{\text{mc}}$  obtained from the deconvolution analysis of the WAXD data and the invariant  $Q$  from the SAXS data are made in Fig. 6a and b at 128.6°C for 32 and 120 K PE samples, respectively. The development of the crystallinity appears to lag behind the invariant  $Q$  consistently. The period of the time lag is indicated by two dotted lines, which represent the apparent onset time for the initial appearance of the SAXS peak ( $t_{\text{SAXS}}$ ) and the apparent onset time for the minimum measurable crystallinity from the crystal reflection (110) in WAXD ( $t_{\text{WAXD}}$ ). It is found that the lag time ( $t_{\text{WAXD}} - t_{\text{SAXS}}$ ) decreases with decreasing crystallization temperature or increasing degree of supercooling. Furthermore, this lag is found to increase with the increase in molecular weight, due to the slower crystallization rate of the higher molecular weight polymer. These results are in general agreement with the data reported in *iPP* [9–11].

The ‘induction period’ can be defined as the period between the starting time of the measurement ( $t_0$ ) and the apparent onset time for WAXD ( $t_{\text{WAXD}}$ ). This period is associated with the characteristic time to grow crystals from the amorphous state to the level of detectable crystallinity. Prior to  $t_{\text{SAXS}}$ , no excess SAXS profile can be measured. After  $t_{\text{SAXS}}$ , a discrete SAXS maximum is seen in the profile, whose intensity increases dramatically with time (Fig. 6a and b). Discrete scattering profiles observed during the period between  $t_{\text{SAXS}}$  and  $t_{\text{WAXD}}$  have been reported also in *iPP* [9–11]. Ryan et al. have used the method of the spinodal decomposition to analyze their SAXS data since the peak intensity grew exponentially with time, while the peak position remained constant. This behavior is considered to be the characteristic of the spinodal decomposition at the early and the intermediate stages of crystallization. When the decomposition is in the late stage, the domains would continuously coarsen with time, shifting the peak position to lower values of  $q$ . If the method of the spinodal decomposition as outlined by Ryan et al. is used, we can extract similar trends of results as reported in *iPP* [9,10]. After careful examination of our data, however, we decided that the spinodal decomposition approach might be inappropriate for the analysis due to the following reason. It is seen that despite the increase in scattering intensity, the scattering peak



(a)

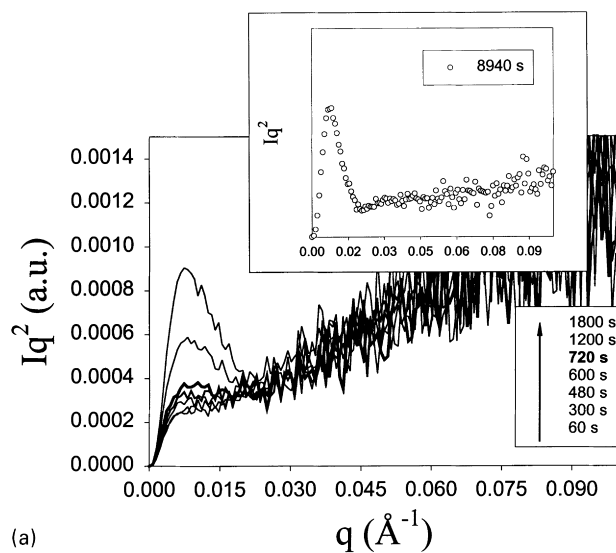


(b)

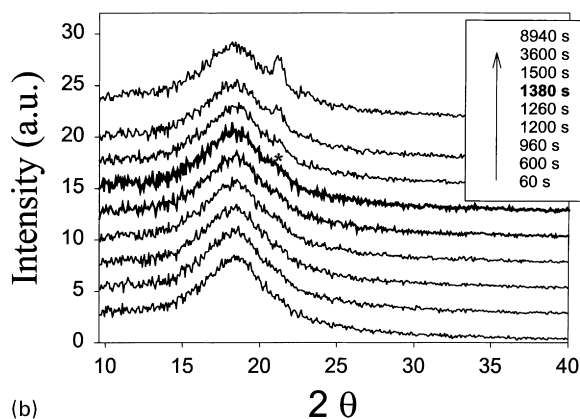
Fig. 3. Selected (a) SAXS; (b) WAXD profiles collected during isothermal crystallization of 32 K PE at 128.6°C for the comparison of the initial appearance of the SAXS peak and the WAXD crystal reflections. (The bold line indicates the initial appearance.)

position is not shifted to lower  $q$  values at long times. At very early times the data even suggest a slight increase in  $q$  (with time), indicating a decrease of the correlation length or the long period. In Fig. 7, the long period values directly calculated from Bragg's law,  $L_b$ , for 32 K PE at two different temperatures are shown. A trend of slight decrease with time is seen, which is consistent with the results from isothermal crystallization of other polymers [12,16,21,22].

A comparison of the apparent onset times determined by SAXS and WAXD techniques is shown in Fig. 8. It is interesting to see that at a given temperature, the following order always exists:  $t_{\text{WAXD}} > t_{\text{SAXS}}$ . This observation is of course consistent with the notion that large density fluctuations (by SAXS) are detected before the 3D crystal ordering (by WAXD). However, we feel that the apparent delay in WAXD can be attributed to the lesser detection limit ( $\sim 1\%$ ). The SAXS technique clearly has a better detection limit ( $\sim 0.1\%$ ) than WAXD [11]. At this point, we would like to address a different question i.e. whether the initial SAXS and



(a)



(b)

Fig. 4. Selected (a) SAXS; (b) WAXD profiles collected during isothermal crystallization of 120 K PE at 128.6°C for the comparison of the initial appearance of the SAXS peak and the WAXD crystal reflections. (The bold line indicates the initial appearance.)

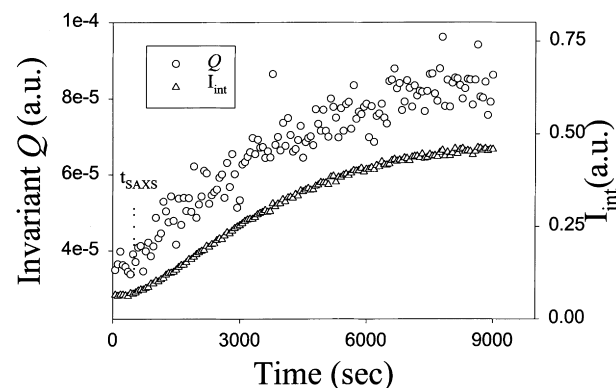


Fig. 5. Time-evolution of the invariant  $Q$  and the integrated intensity  $I_{\text{int}}$  from the SAXS data during isothermal crystallization of 120 K PE at 128.6°C. The apparent onset time ( $t_{\text{SAXS}}$ ) is determined using an interception method.

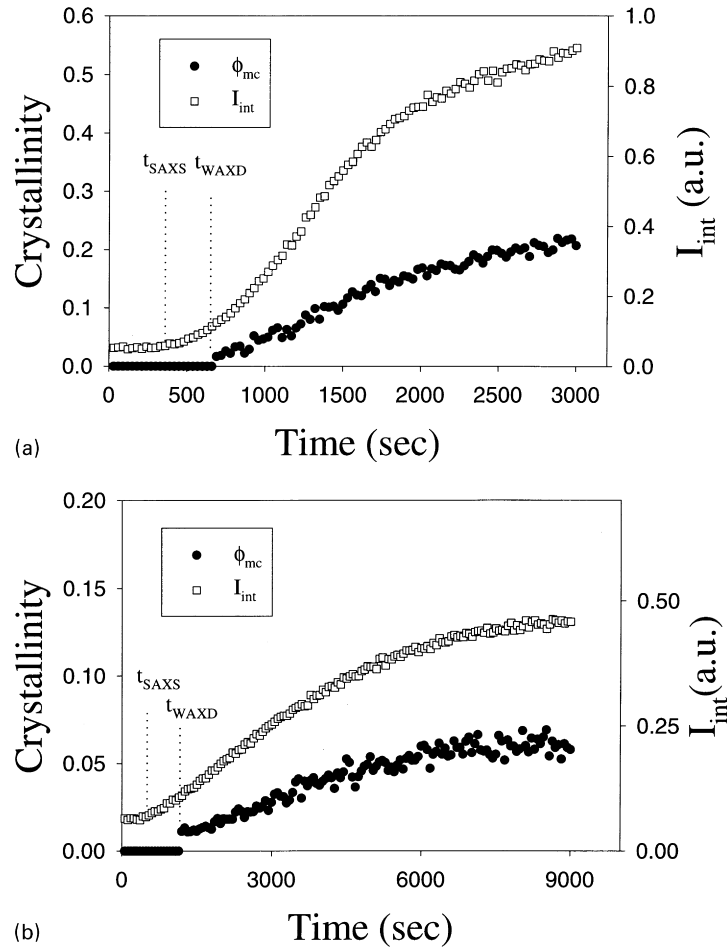


Fig. 6. Time-evolution of the invariant  $Q$  and the crystallinity  $\phi_{mc}$  during isothermal crystallization of (a) 32 K; (b) 120 K PE at 128.6°C. The two dotted lines represent the values of  $t_{SAXS}$  and  $t_{WAXD}$ .

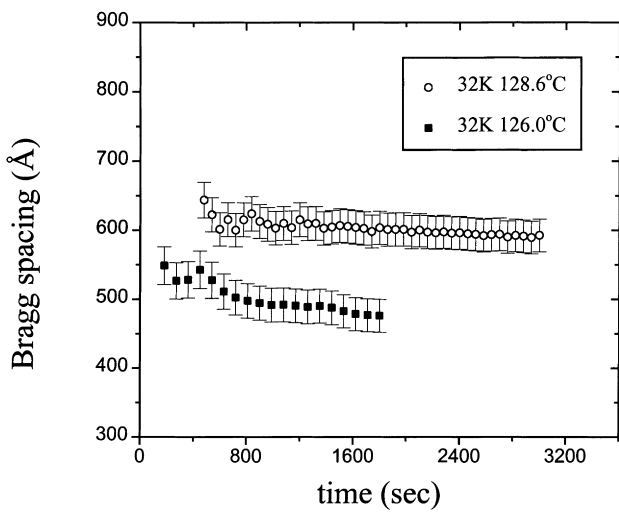


Fig. 7. Time evolution of the long period from Bragg's law,  $L_0$  of 32 K PE at 126.0 and 128.6°C.

WAXD data can be described also by the classic behavior of nucleation and growth using a simple Avrami form.

We have shown that WAXD can give an absolute measure of the crystallinity of the sample. While SAXS (as performed here) does not allow an absolute determination of the crystallinity, we can make some approximations to estimate the level of crystalline fractions. We can assume that the integrated intensity from SAXS ( $X_{SAXS}$ ) is linearly proportional to the crystallinity. This approximation should be good as long as the total crystallinity is low, but it will break down when the primary crystallization is complete and interlamellar regions begin to crystallize. However, in the early stages, the approximation should be quite reasonable. Here, we choose to use the integrated intensity instead of the invariant (Fig. 5), since it has better statistics. We also consider an Avrami form for the crystallinity with an exponent of  $n$  ( $2 < n < 4$ ) and a time constant, which will depend on temperature. The Avrami crystallinity considered here has the form:  $X_{AVRAMI} = 1 - \exp(-(t/\tau)^n)$ . Plotted in Fig. 9a–c are the WAXD crystallinity, the SAXS crystallinity  $X_{SAXS}$ , and the Avrami fit  $X_{AVRAMI}$ . From these figures, we can conclude that the actual detection limit for

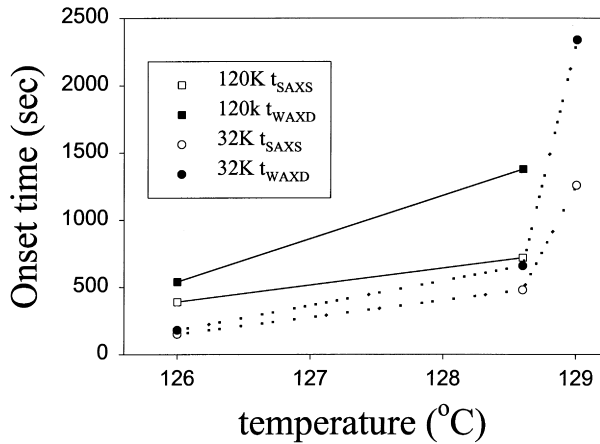


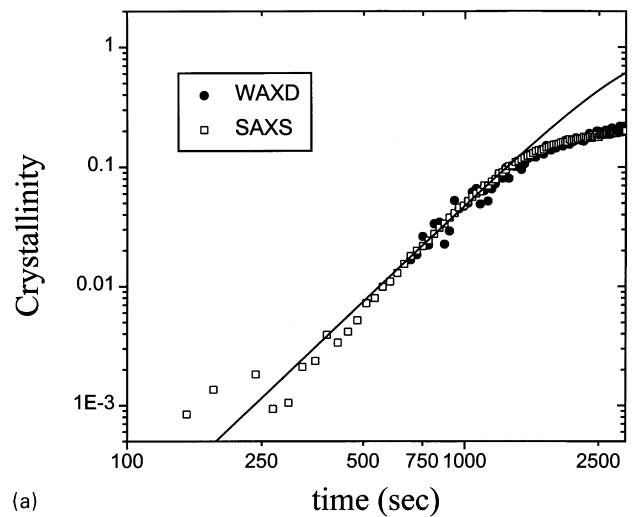
Fig. 8. The comparison of the apparent onset time for SAXS and WAXD for 32 K PE and 120 K PE at different crystallization temperatures.

WAXD is about 1% (the lowest points where finite crystallinity could be extracted and where it still follows the Avrami form) that is the same value as obtained by the model solution study [11], and for SAXS is  $\sim 0.2\%$ . It is clear that the crystallinity data (SAXS and WAXD) in Fig. 9 is consistent with a single Avrami form at the early stages of crystallization.<sup>1</sup> The deviation between the measured data and the Avrami form is seen only at high degrees of crystallinity. This may be explained with two reasons. (1) As the growing objects begin to interact with each other, we expect a breakdown of the approximation relating the scattering intensity to the volume crystallinity. (2) The process of secondary crystallization may follow a different Avrami form. In general, we find that the SAXS data follows the initial Avrami form at very early times which is limited only by the noise level (0.2%). From Fig. 9, we can conclude that SAXS and WAXD data collected at the early stages of crystallization are consistent with the Avrami behavior.

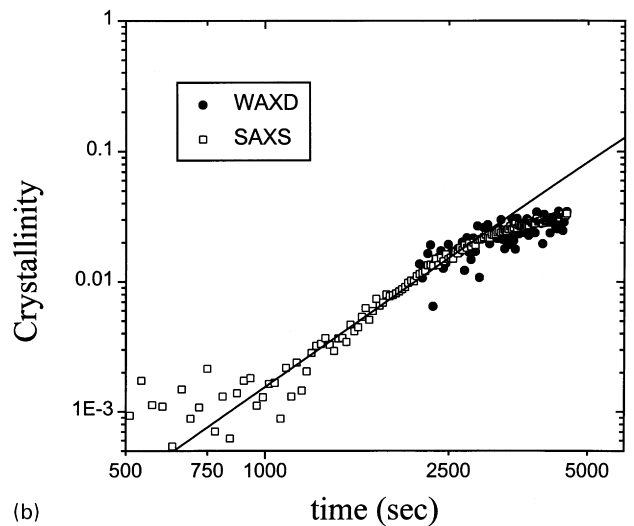
#### 4. Conclusions

The early stages of melt crystallization in fractionated PE were studied by simultaneous SAXS and WAXD measurements with synchrotron radiation. During the early stages of crystallization, we found that the SAXS peak corresponding to density fluctuations with an average spacing of 40–80 nm was present prior to the detection of 3D crystal ordering by WAXD. The lack of any increase in the spacing or invariant with time argues against the hypothesis of the spinodal decomposition in the supercooled melt. Making trivial assumptions relating SAXS to volume fraction of an ordered

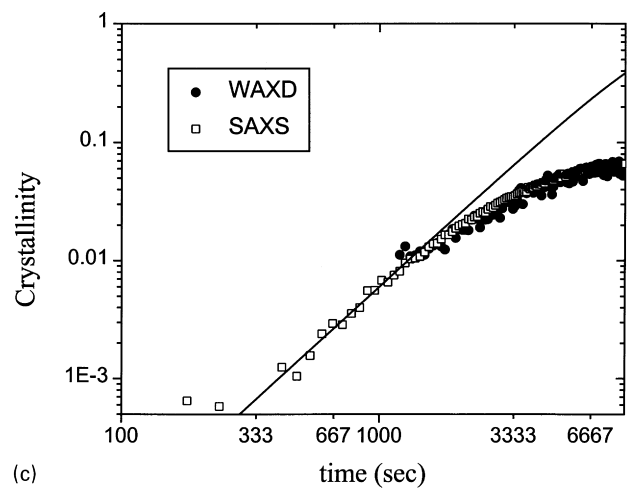
<sup>1</sup> The Avrami constants for the 32 K PE sample at different temperatures are about the same (2.5 and 2.7). The larger time constant at the higher crystallization temperature indicates a slower crystallization rate. The Avrami constant for the high molecular weight PE was found to be lower (2.0).



(a)



(b)



(c)

Fig. 9. Time evolution of relative crystallinity from WAXD, SAXS and the fitted Avrami equation for PE 32 K at (a) 128.6°C (Avrami parameters:  $\tau = 3060$  s,  $n = 2.7$ ); (b) 129.0°C (Avrami parameters:  $\tau = 13,280$  s,  $n = 2.5$ ); (c) PE 120 K at 128.6°C (Avrami parameters:  $\tau = 12,280$  s,  $n = 2.0$ ), respectively.

phase, the WAXD and the SAXS data are found to follow a simple Avrami form in the early stages of crystallization, which indicates that the early stages of crystallization can be described with the conventional nucleation and growth theories. From this study, we conclude that the WAXD technique can detect a minimum degree of crystallinity of about 1%, while the SAXS technique detects crystallinity of about 0.2%. The observation of the kinetics discrepancy between SAXS and WAXD may mainly be due to the differences in the detection limit of the different techniques.

### Acknowledgements

The authors gratefully acknowledge Dr Fengji Yeh and Dr Lizhi Liu (SUNYSB) for providing assistance during synchrotron measurements. The authors are indebted to the helpful discussions with Profs Stephen Z. D. Cheng, Benjamin Chu, Andrew Keller, Bernard Lotz, Richard S. Stein and Jerold M. Schultz. The financial support of this work was provided by a grant from NSF (DMR 9732653). The DOE grant (DE-FG02-99ER45760) for the support of the Advanced Polymers Beamline is also acknowledged. The NSLS at BNL is supported by the US Department of Energy.

### References

- [1] Lee CH, Saito H, Inoue T, Nojima S. *Macromolecules* 1996;29:7034.
- [2] Imai M, Mori K, Mizukami T, Kaji K, Kanaya T. *Polymer* 1992;33:4451.
- [3] Imai M, Kaji K, Kanaya T, Sakai Y. *Physical Review B* 1995;52:12,696.
- [4] Imai M, Mori K, Mizukami T, Kaji K, Kanaya T. *Polymer* 1992;33:4457.
- [5] Imai M, Kaji K, Kanaya T. *Macromolecules* 1994;27:7103.
- [6] Ezquerro TA, López-Cabarcos E, Hsiao BS, Baltà-Calleja FJ. *Phys Rev E* 1996;54:989.
- [7] Cahn JW, Hilliard JE. *J Chem Phys* 1958;28:258.
- [8] Cahn JW. *J Chem Phys* 1965;42:93.
- [9] Terrill NJ, Fairclough PA, Towns-Andrews E, Komanschek BU, Young RJ, Ryan AJ. *Polymer* 1998;39(11):2381.
- [10] Ryan AJ, Fairclough PA, Terrill NJ, Olmsted PD, Poon WCK. *Faraday Discuss* 1999;112:13.
- [11] Wang ZG, Hsiao BS, Sirota EB, Agarwal P, Srinivas S. *Macromolecules* 2000;33:978.
- [12] Wang ZG, Hsiao BS, Sauer BB, Kampert WG. *Polymer* 1999;40:4615.
- [13] Olmsted PD, Poon WCK, McLeish TCB, Terrill NJ, Ryan AJ. *Phys Rev Lett* 1998;81:373.
- [14] Avrami MJ. *J Chem Phys* 1939;7:1103.
- [15] Hsiao BS, Chu B, Yeh F. *NSLS July Newsletter* 1997:1 (<http://bnlx27c.nsls.bnl.gov>).
- [16] Hsiao BS, Gardner KH, Wu DQ, Chu B. *Polymer* 1993;34(19):3996.
- [17] Glatter O, Kratky O. *Small-Angle X-ray Scattering*, New York: Academic Press, 1982. p. 242 (chap 8).
- [18] Strobl GR, Schneider M. *J Polym Sci, Polym Phys Ed* 1980;18:1343.
- [19] Baltà-Calleja FJ, Vonk GG. *X-ray Scattering of synthetic polymers*. New York: Elsevier, 1989.
- [20] Wunderlich B. *Molecular physics*, vol. 2. New York: Academic Press, 1979.
- [21] Verma RK, Hsiao BS. *Trends in Polymer Sciences* 1996;4(10):312.
- [22] Verma RK, Marand H, Hsiao B. *Macromolecules* 1996;29:7767.